Sensors and Materials, Vol. 34, No. 8 (2022) 2911–2928
MYU Tokyo

S & M 3014

Inertial Measurement Unit-sensor-based Short Stick Exercise Tracking to Improve Health of Elderly People

Kazuki Oi,[1] Yugo Nakamura,[2,3*] Yuki Matsuda,[1,3]
Manato Fujimoto,[4] and Keiichi Yasumoto[1]

[1]Nara Institute of Science and Technology, Ikoma, Nara 630-0192, Japan
[2]Kyushu University, Fukuoka, Fukuoka 819-0395, Japan
[3]JST PRESTO, Tokyo 102-0076, Japan
[4]Osaka Metropolitan University, Osaka, Osaka 558-8585, Japan

(Received May 11, 2022; accepted July 5, 2022)

Keywords: short stick exercise, machine learning, IMU

Short stick exercises have been attracting attention from the viewpoint of preventing falls and improving the health of elderly people and are generally performed under the guidance of instructors and nursing staff at nursing homes. However, in situations such as the COVID-19 pandemic, where people should refrain from unnecessary outings, it is advisable that individuals perform short stick exercises at home and record their exercise implementation status. In this paper, we propose an inertial measurement unit (IMU)-sensor-based short stick exercise tracking method that can automatically record the types and amounts of exercises performed using a short stick equipped with an IMU sensor. The proposed method extracts time-domain and frequency-domain features from linear acceleration and quaternion time-series data obtained from the IMU sensor and classifies the type of exercise using an inference model based on machine learning algorithms. To evaluate the proposed method, we collected sensor data from 21 young subjects (in their 20s) and 14 elderly subjects (79–95 years old), where the participants performed three sets (10 times per set) of eight basic types of short stick exercises (five types for elderly people). As a result of evaluating the proposed method using this data set, we confirmed that when LightGBM was used as the learning algorithm, it achieved *F* values of 90.0 and 86.6% for recognizing the type of exercise for young and elderly people, respectively.

1. Introduction

Falls in elderly people often result in fractures and other serious injuries that require hospitalization and can lead to people becoming bedridden. Therefore, it is important to engage in regular moderate exercise to prevent falls. In recent years, short stick exercises, which are simple and easy to perform, have been attracting attention for the purpose of preventing falls and improving the health of elderly people.(1) These exercises are generally performed at nursing homes and other institutions under the direct supervision of instructors and caregivers.

*Corresponding author: e-mail: y-nakamura@ait.kyushu-u.ac.jp
https://doi.org/10.18494/SAM3968

ISSN 0914-4935

However, in the current COVID-19 pandemic, where people are urged to refrain from going out unnecessarily, it is desirable for individuals to perform and record short stick exercises on their own. Therefore, a means by which users can easily record how many short stick exercises they have performed of each type at home is necessary.

In existing research on exercise support, Shen *et al.*[2] developed MiLift, a smartwatch-based system that can track cardio and weightlifting workouts with high accuracy. Focusing on weight training without equipment, Takata *et al.*[3] investigated the recognition accuracy of 10 different exercises for each position of a wearable sensor. As a result, a 93.5% recognition accuracy was achieved when the sensor was placed on the wrist and the waist. Although these studies achieved highly accurate motion recognition with body-worn IMU sensors, they did not examine methods for short stick exercises.

In this study, we investigate an approach to identify the types of short stick exercises performed by users using only one sensor, an inertial measurement unit (IMU) sensor attached to a stick used to perform short stick exercises. Our goal is to realize a support system for short stick exercises that can automatically record the types of short stick exercises performed by elderly people and how many they perform and provide feedback to improve the movement for each exercise.

In this paper, as a first step toward realizing such a support system, we propose an IMU-based short stick exercise tracking method that can automatically record the type and number of each exercise while a person performs exercises using a short stick equipped with an IMU sensor. The proposed method extracts time-domain and frequency-domain features from linear acceleration and quaternion time-series data obtained from the IMU sensor and classifies the type of exercise using an inference model based on machine learning algorithms.

In the experiment, sensor data were collected from 21 young participants (in their 20s) for eight basic types of exercise and 14 elderly participants (79–95 years old) for five types of exercise. We evaluated the performance of the proposed method using the collected sensor data. As a result, we confirmed that when LightGBM was used as the learning algorithm in the leave-one-person-out scenario, it achieved F values of 90.0 and 86.6% for recognizing the type of exercise for young and elderly participants, respectively. The results demonstrate that our proposed method works well for a variety of short stick exercises for both young and elderly people.

2. Related Work

In this section, we describe related research on health support for elderly people and research on exercise support. Dobre *et al.* developed a system that provides non-intrusive monitoring and support for elderly people to enhance the provision of professional healthcare,[4] and Richard *et al.* proposed a health management system that displays temperature and heart rate data on a liquid crystal display (LCD) and sends automatic notifications to caregivers and doctors.[5] This system immediately detects any physical abnormality in elderly people and enables a rapid response. A method to monitor the behavior of elderly people living alone and detect deviations from past behavior patterns has also been proposed by Susnea *et al.*[6]

Voicu *et al.* proposed a human physical activity recognition system based on data collected from smartphone sensors.(7) It extracts relevant features from six categories: walking, running, sitting, standing, climbing, and descending. Evaluation of the collected data showed that most activities were correctly recognized, with four of them achieving an average accuracy of 93%.

Kurban *et al.* proposed a daily motion recognition system using a tri-axis acceleration sensor that can be used in various body positions.(8) With this system, walking, sitting, standing, jumping, and falling motions are collected from subjects. Principal component analysis is used as the feature analysis method for classification, and the proposed method achieves a maximum accuracy of 100% and an average accuracy of 96.54%.

Shen *et al.* developed MiLift, which can track cardio and weightlifting workouts with high accuracy using a smartwatch.(2) The system achieved over 90% accuracy and repeatability in tracking both aerobic and weightlifting exercises. Takata *et al.* also focused on weight training without equipment and investigated the recognition accuracy of 10 different exercises for each position of a wearable sensor.(3) As a result, they reported that the waist was the optimal position when one sensor was used, and when two sensors were placed at both the wrist and the waist, the weight training exercise was recognized with a high accuracy of 93.5%. Turmo *et al.* developed a system that uses 3D-printed wearable projection lights to visually assist the user in performing correct motor movements.(9)

Torigoe *et al.* proposed a method to detect and recognize five types of striking motions in kendo by attaching IMU sensors to the wrist, waist, shinai flange, and shinai tip. They analyzed inertial sensor data of striking motions of experienced and inexperienced kendo players and reported that the proposed method based on dynamic-time warping could detect striking motions with an F value of 89.9%.(10) Blank *et al.* attached inertial sensors to table tennis rackets and collected data on eight basic stroke types from 10 amateur and 10 professional players. First, a single stroke was detected using an event detection algorithm. The features were then computed and used as the input for stroke type classification. They reported a high recognition accuracy of 96.7%.(11) Jensen *et al.* developed a golf putt analysis system using data from an inertial sensor attached to the end of a golf club using off-the-shelf components with removable sensors.(12) The main functions were automatic putt detection by machine learning and real-time parameter calculation in the club coordinate system. The authors also conducted an experiment and reported that eight out of 11 subjects detected more than 83% of putts, while the false positive rate was only 2.4%. Sundholm *et al.* used the Smart-Mat, which incorporates a pressure cloth sensor in an exercise mat, to recognize 10 standard exercises and count and recognize the number of reps.(13) In an experiment conducted by Sundholm *et al.*, in which seven subjects repeated each exercise 20 times, a user-independent recognition rate of 82.5% and a counting accuracy of 89.9% were obtained. Using scaling and shuffling techniques, Lai *et al.* developed a game that can provide tempo variations in strength training while maintaining the training volume and training goals.(14) They conducted a user survey of 24 participants and found that the game was entertaining and enjoyed by the participants.

In this study, we focused on short stick exercises, which have received much attention in recent years for their effectiveness in preventing falls and promoting the health of elderly people. We attached an IMU sensor to a stick used for short stick exercises and attempted to develop a method by which users can automatically record the type and number of exercises they have performed simply by exercising using the stick equipped with the IMU sensor. To our knowledge, no study has focused on short stick exercises performed by elderly people or investigated the applicability of the methods established in previous studies of human activity recognition to the monitoring of short stick exercises.

3. Short Stick Exercise Recognition

In this section, we describe the sensor device used and its attachment position, the exercises recognized in this study, and details of the short stick exercise recognition method.

3.1 Sensor device used and mounting position

We used a MetaMotionR (https://mbientlab.com/metamotionr/) IMU sensor device attached to a short stick. The IMU sensor can perform linear acceleration and quaternion measurements and has a recording rate of up to 100 Hz. It can also collect linear acceleration and quaternion data wirelessly. A quaternion is an extension of the imaginary axis of a complex number to three dimensions. The quaternion value describes the orientation of the sensor. The sensor is embedded in a hole in the center of the stick, as shown in Fig. 1. The exerciser performs the exercise while holding both ends of the stick. In addition, the stick holding and stick angle are consistent.

3.2 Basic exercises as recognition targets

Eight basic exercises were chosen as recognition targets from the short stick exercises introduced in Ref. 1, which are shown in Fig. 2 and explained below.

Exercise A: Stick straddling

The exerciser holds the stick with both hands and straddles the stick without bending it. Next, they lift their hips off the chair and raise the stick to the back of the waist. Finally, they return to their original position in reverse order. This exercise increases the flexibility of the legs and maintains their range of motion.

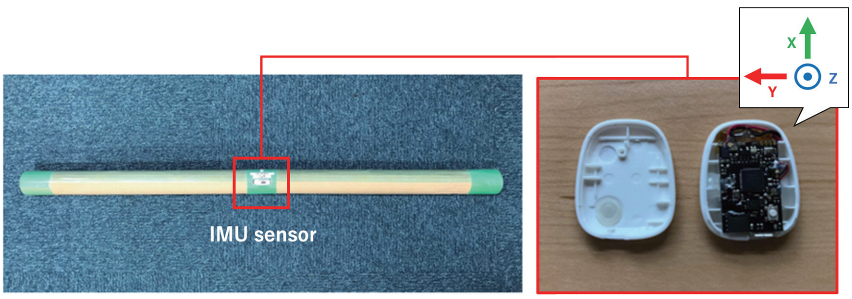

Fig. 1. (Color online) Short stick equipped with an IMU sensor.

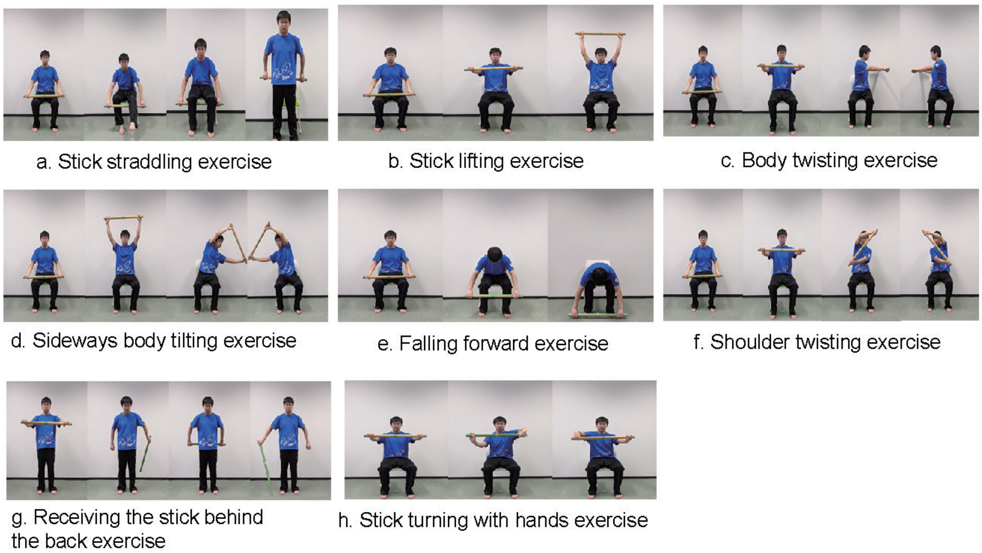

Fig. 2. (Color online) Eight types of short stick exercises.

Exercise B: Stick lifting

The exerciser holds the stick with both hands and does a *banzai* (holding up two hands) with their back straight. They breathe and raise their shoulder during the exercise. This exercise stretches the back and helps prevent falling to the side.

Exercise C: Body twisting

The exerciser stretches backward and rotates their body to the left and right while holding the stick with both hands. Rotating the body helps improve the mobility of the spinal column and thorax and is also a necessary element of getting back to one's feet after losing balance.

Exercise D: Sideways body tilting

The exerciser holds the stick with both hands, stretches backward, and bends their body to the left and right. This exercise helps increase the flexibility of the ribcage.

Exercise E: Falling forward

The exerciser holds the stick with both hands, leans forward, and places the stick on the floor. By doing this exercise, the exerciser loads their weight on the sole of the foot and realizes the forward leaning posture necessary for standing up.

Exercise F: Shoulder twisting

The exerciser holds a stick with both hands and twists their shoulders as if they were turning the stick in front of their body. Twisting the shoulders can increase the mobility of the shoulders.

Exercise G: Receiving the stick behind the back

The exerciser passes the stick behind their back and receives it with the opposite hand. Manipulating the stick in an unseen location enhances body movement imagery and increases shoulder mobility.

Exercise H: Stick turning with hands

The exerciser holds the stick with both hands and rotates it by moving the wrists up and down alternately. This exercise can increase the mobility and flexibility of the wrists.

3.3 Observation of sensor data waveform for each type of exercise

Figure 3 shows typical sensor data waveforms; the composite acceleration and quaternion, which are the combined *x*-, *y*-, and *z*-axis accelerations for each exercise, are shown in the figure. The horizontal axis represents the time and the vertical axis represents the magnitude of the composite acceleration and quaternion.

As shown in Fig. 3(a), the above waveforms show that the composite acceleration for Exercise A has some spikes. This is probably due to a foot hitting the stick. On the other hand, the quaternions show no significant changes in the *w*-, *x*-, *y*-, and *z*-components. This may be due to the nature of the basic movement of exercise A, which does not involve large stick movements.

As shown in Fig. 3(b), the composite acceleration for Exercise B has two points where it is large. This is because the arm is larger when it is raised and when it is lowered. Also, the magnitudes of the *w*- and *y*-components of the quaternion decrease during the banzai. This is thought to be due to the fact that the *y*-component decreases when the stick is raised.

As shown in Fig. 3(c), the composite acceleration for Exercise C shows a large overall change. We believe this is due to the large and fast movement of raising the stick to chest height, twisting the body to the left or right, and returning to the original position. The quaternion sometimes has a large *z*-component and sometimes has a small *z*-component. This is thought to be the result of twisting to the left or right.

As shown in Fig. 3(d), the composite acceleration for Exercise D shows no significant change overall. This is due to the fact that although the movements in this exercise are large, it is difficult to move the body quickly. In the quaternion, the *x*-component decreases as the *z*-component increases, and the *x*-component increases as the *z*-component decreases. This is thought to be due to the increase in the *z*-component when the body is tilted to the left or right.

As shown in Fig. 3(e), the composite acceleration for Exercise E is generally small. This is because this exercise only involves bringing the stick from the sitting position to the knee height to the foot height, and therefore the stick is not moved quickly. The quaternion shows that the *y*-component increases during the exercise. This is because the *y*-component increases after the arms are lowered and returns to its original magnitude when the arms return to their original position.

As shown in Fig. 3(f), the composite acceleration for Exercise F shows a large change from the beginning to the end of the exercise. This is thought to be due to the fact that this exercise starts at knee height, moves to chest height, twists to the left or right, and then returns to the original knee height, making it easy to move the stick quickly. The quaternion has a point where the *x*-component decreases as the z-component increases and the *x*-component increases as the *z*-component decreases. This is thought to be due to the fact that the change in the *z*-component increases when the shoulder is twisted to the left or right.

As shown in Fig. 3(g), the composite acceleration for Exercise G shows a small overall change. This may be because the exerciser cannot see the stick, and therefore, if the movement is made faster, the exerciser may find it more difficult to perform the exercise. In the quaternion, the *y*-component increases when the exercise begins and returns to its original value when the exercise ends. This is because the stick is lowered with the left hand, received with the right hand, and returned to its original position.

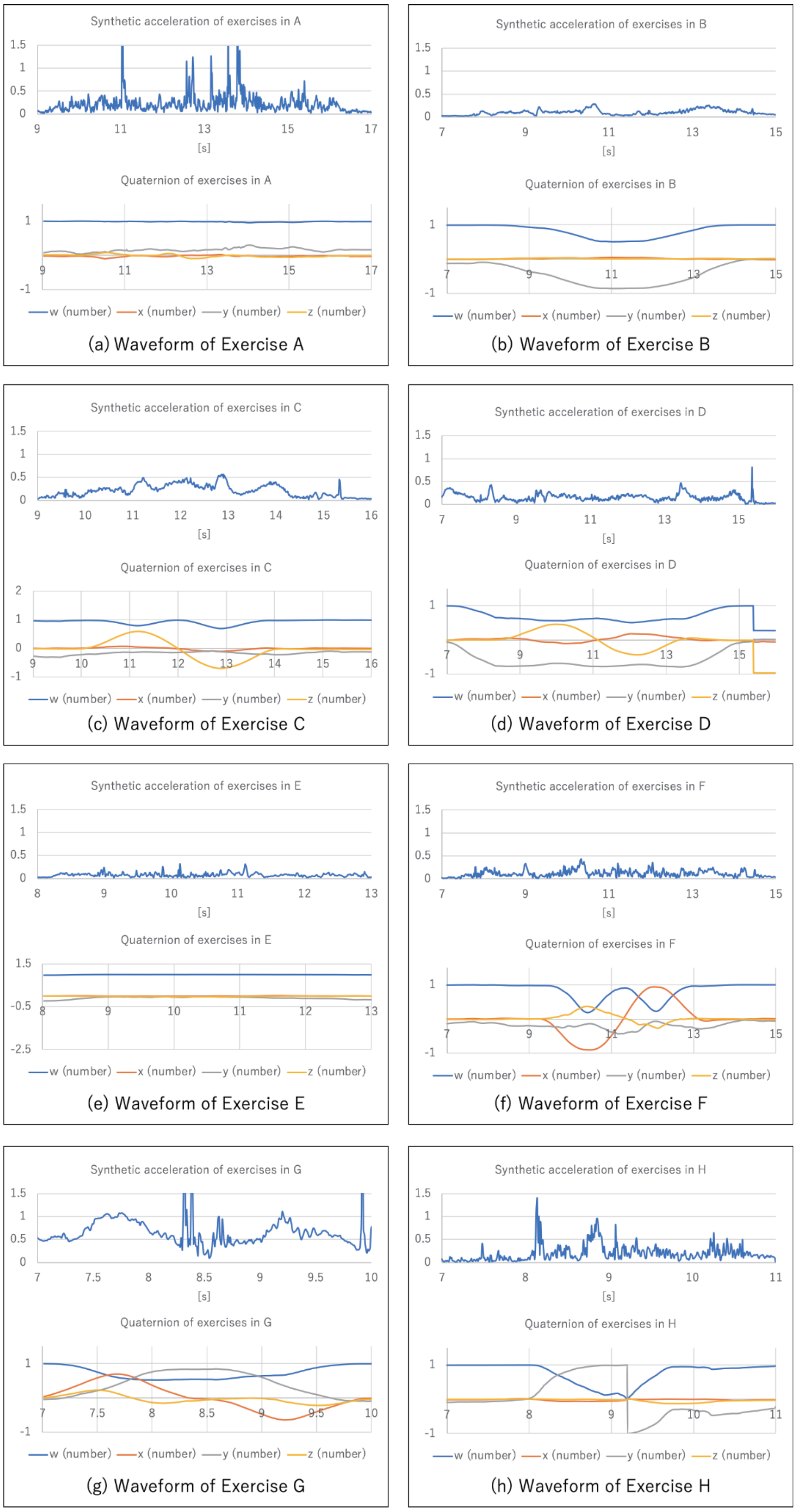

Fig. 3. (Color online) Sensor waveforms.

As shown in Fig. 3(h), the composite acceleration for Exercise H has two points where the acceleration is larger. This is due to the division of the stick into two separate movements when it is turned. The quaternion shows that the y-component is larger in some areas and smaller in others. This is because the y-component increases when the first turn is made from the left-hand side and then decreases when the next turn is made from the right-hand side.

3.4 Proposed method

Our aim is to develop a method to automatically record the type and number of each short stick exercise performed by elderly people. Specifically, an IMU sensor is attached to the short stick, and the sensor data (linear acceleration and quaternion) obtained from it is analyzed to classify the type of motion automatically.

An overview of the proposed method is shown in Fig. 4. The linear acceleration (x-, y-, z-components, synthetic value) and quaternion (w-, x-, y-, z-components, synthetic value) are obtained from the IMU sensor. Here, the sampling rate is 100 Hz. In this study, data preprocessing and feature extraction are performed in accordance with the findings of existing studies;[10,15] we apply a sliding window with a window size of 1.28 s (1 window = 128 samples) and a step size of 0.64 s. We first apply a noise reduction process to nine different time-series data using a 0.3 s median filter. Next, we separate the sensor data into time-domain and frequency-domain series using a Fast Fourier transform. Then, feature extraction processes based on the 17 functions (mean, std, mad, max, min, energy, entropy, iqr, autoregression, range, rms, skewness, kurtosis, maxFreqInd, meanFreq, energyBand, psd) shown in Table 1 are applied to the time-domain and frequency-domain series. Through these processes, a 225-dimensional feature vector is generated from one window of sensor data. Our method uses a recognition model based on machine learning to infer the type of short stick exercise for this feature vector. The machine learning models used for the exercise recognition include nine typical machine learning algorithms [support vector machine (SVM), artificial neural network (ANN), random forest (RF), decision tree (DT), LightGBM, logistic regression (LR), k-nearest neighbor (KNN), naive Bayes (NB), extra-trees (ET)]. In the implementation, we train each model using the default parameters of the scikit-learn and LightGBM packages.

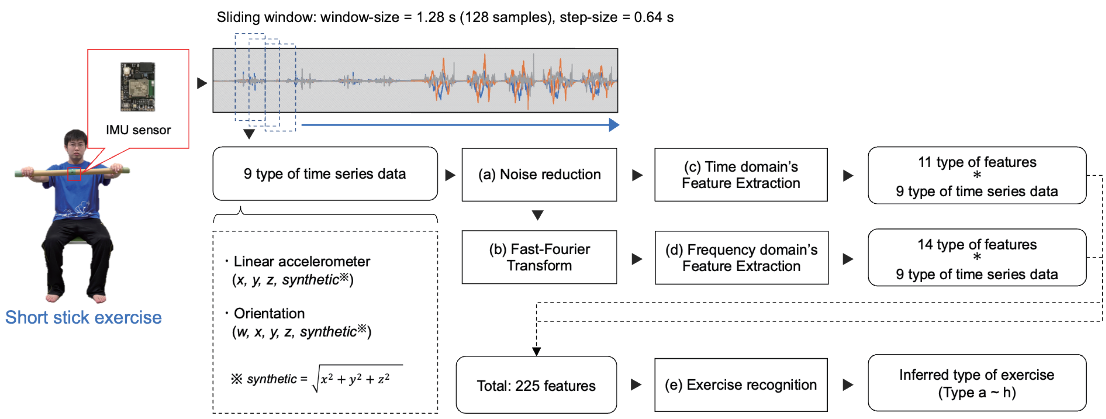

Fig. 4. (Color online) Overview of proposed method.

Table 1
Feature list for short stick exercise recognition.

Function	Description	Formulation	Type
mean（s）	Arithmetic mean	$\bar{s} = \frac{1}{N}\sum_{i=1}^{N} s_i$	T，F
std（s）	Standard deviation	$\sigma = \sqrt{\frac{1}{N}\sum_{i=1}^{N}(s_i - \bar{s})^2}$	T，F
mad（s）	Median absolute deviation	$median_i(\mid s_i - median_j(s_j) \mid)$	T，F
max（s）	Largest values in array	$max_i(s_i)$	T，F
min（s）	Smallest value in array	$min_i(s_i)$	T，F
energy（s）	Average sum of the square	$\frac{1}{N}\sum_{i=1}^{N} s_i^2$	T，F
entropy（s）	Signal Entropy	$\sum_{i=1}^{N}(c_i \log(c_i)), c_i = s_i / \sum_{j=1}^{N} s_j$	T，F
iqr（s）	Interquartile range	$Q3(s) - Q1(s)$	T，F
autorregresion（s）	4th order Burg Autoregression coefficients	$a = arburg(s,4), a \in R^4$	T
range（s）	Range of smallest value and Largest value	$max_i(s_i) - mix_i(s_i)$	T
rms（s）	Root square means	$\sqrt{\frac{1}{N}(s_1^2 + s_2^2 + \cdots + s_N^2)}$	T
skewness（s）	Frequency signal Skewness	$E[(\frac{s-\bar{s}}{\sigma})^3]$	F
kurtosis（s）	Frequency signal Kurtosis	$E[(s-\bar{s})^4]/E[(s-\bar{s})^2]^2$	F
maxFreqInd（s）	Largest frequency component	$argmax_i(s_i)$	F
meanFreq（s）	Frequency signal weighted average	$\sum_{i=1}^{N}(is_i)/\sum_{j=1}^{N} s_j$	F
energyBand（s，a，b）	Spectral energy of a frequency band [a, b]	$\frac{1}{a-b+1}\sum_{i=a}^{b} s_i^2$	F
psd（s）	Power spectral density	$\frac{1}{Freq}\sum_{i=1}^{N} s_i^2$	F

N : signal vector length，Q : Quartile，T : Time domain features, F : Frequency domain features.

4. Evaluation Experiment

To investigate the effectiveness of the proposed method, we conducted a data collection experiment with 21 young people in their 20s and 14 elderly people (ages 79–95 who require nursing care). In the experiment with elderly subjects, an instructor performed the short stick exercise in front of them and asked them to imitate him, as shown in Fig. 5.

The subjects held the Smart Stick shown in Fig. 4 and performed three sets (10 times per set) for each of the eight targeted exercises (five exercises (Exercises B to F) for the elderly people due to their physical problems after consulting with caregivers), and the measurement data were collected. The data included linear acceleration and quaternion data obtained from the IMU sensor.

Owing to the significant differences in athletic performance between young people and the elderly, the characteristics of the obtained sensor data can differ significantly. To clarify the difference between the two, we collected sensor data from both groups. From the viewpoint of improving the accuracy of the recognition model, we plan to train different exercise recognition models for young and elderly people and design a method to adaptively select the model to be used according to the user's ability. Therefore, in this experiment, we also proceeded with a survey on the type of features that are effective for automatically classifying healthy and elderly people.

Fig. 5. (Color online) Scene from data collection experiment.

4.1 Comparison of sensor waveforms between young and elderly people

The sensor waveforms (linear acceleration and quaternion) of five types of exercises (Exercises B to F) performed by elderly subjects were compared with those of the same exercises performed by young people.

Figure 6 shows the sensor waveforms of a young person and an elderly person performing Exercise B. The composite acceleration of elderly people is generally smaller than that of young people. This is thought to be due to the slower movements of elderly people. The quaternion of the young person also shows a decrease in both the *w*- and *y*-components, but only the y-component shows a decrease for the elderly people. This may be due to the fact that the arms of the elderly people were raised less than those of the young people.

Figure 7 shows the sensor waveforms of a young person and an elderly person performing Exercise C. The sensor waveforms show that the acceleration of elderly people is smaller. This indicates that the movement is slow. Next, the quaternions are compared. The young person's quaternion has an inverse S-shaped *z*-component, while the elderly person's quaternion has an inverse S-shaped *z*-component and other components. This is thought to be due to the inability to keep the bar horizontal.

Figure 8 shows the sensor waveforms of a young person and an elderly person performing Exercise D. The sensor waveforms show that the acceleration of the elderly person is lower. The quaternion waveforms are similar.

Figure 9 shows the sensor waveforms of a young person and an elderly person performing Exercise E. The sensor waveforms show that the acceleration is small for both people but is large in some areas. This is thought to be due to the stick hitting the knee during the exercise. The quaternion shows that the *y*-component increases during the exercise for both the young and elderly people. This is thought to be due to the correct lowering of the stick.

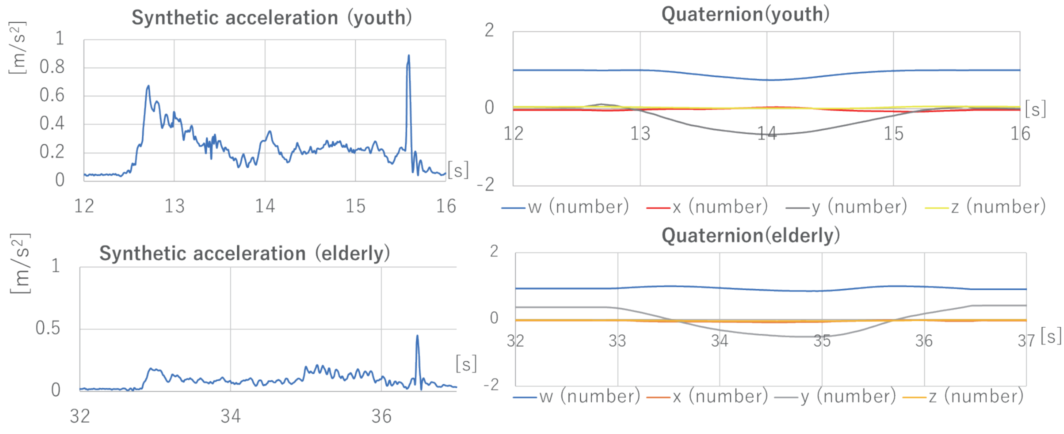

Fig. 6. (Color online) Comparison of waveforms in Exercise B.

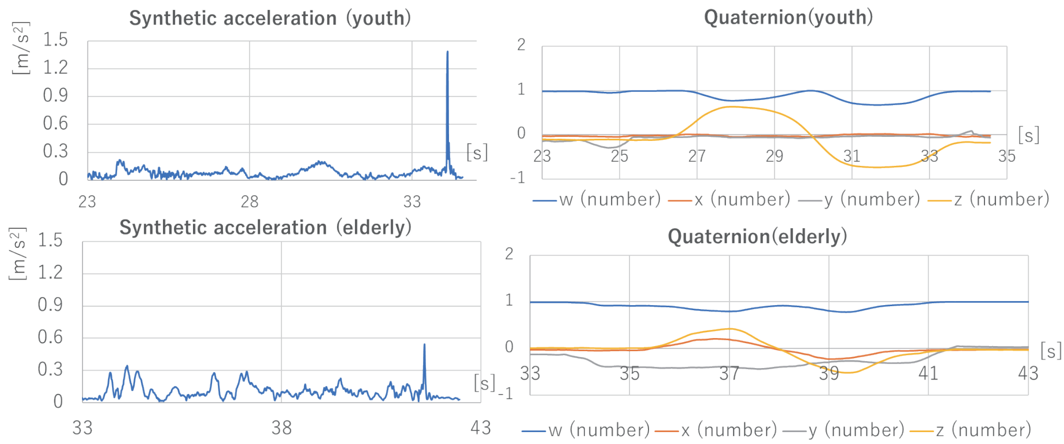

Fig. 7. (Color online) Comparison of waveforms in Exercise C.

Figure 10 shows the sensor waveforms of a young person and an elderly person performing Exercise F. The sensor waveforms show that acceleration is generally small for both people. However, the acceleration of the elderly person is higher in some areas. This is thought to be caused by the stick hitting the knee during the exercise. The quaternions have S-shaped *w*- and *x*-components for both the young and elderly people, but the waveform of the elderly person is less smooth than that of the young person. This may be because the movements of elderly people are less smooth than those of young people.

4.2 Significantly different features for young and elderly people

In this study, we examined features that are useful in automatically determining which age group people exercised. The results revealed that the data for the young and elderly people did not correspond and did not follow a normal distribution. Therefore, a Mann–Whitney test was performed, which examines whether there is a difference between the two groups of uncorrelated data. The results showed that the composite acceleration mean (acc_t-Mean-mag) in the time domain was particularly significantly different between the two groups. The details are described below.

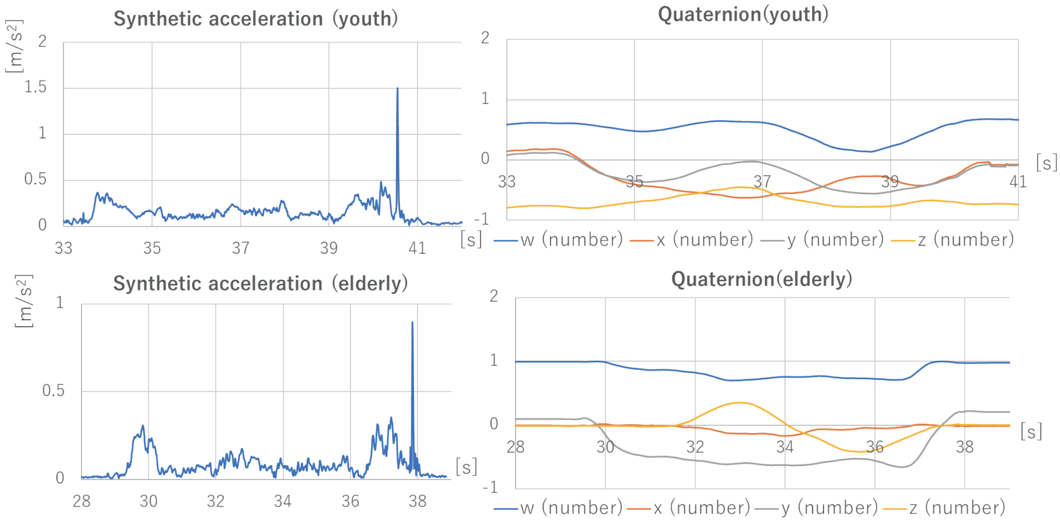

Fig. 8. (Color online) Comparison of waveforms in Exercise D.

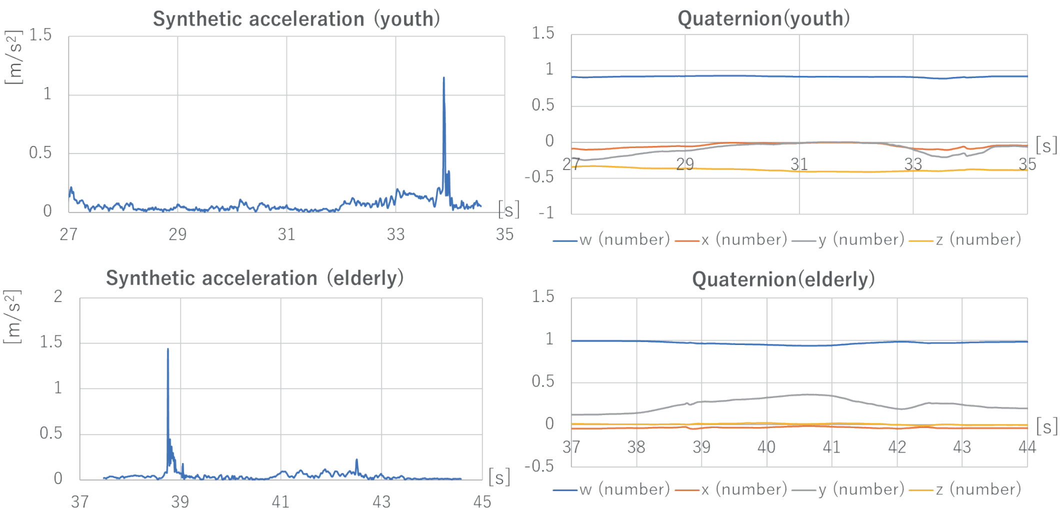

Fig. 9. (Color online) Comparison of waveforms in Exercise E.

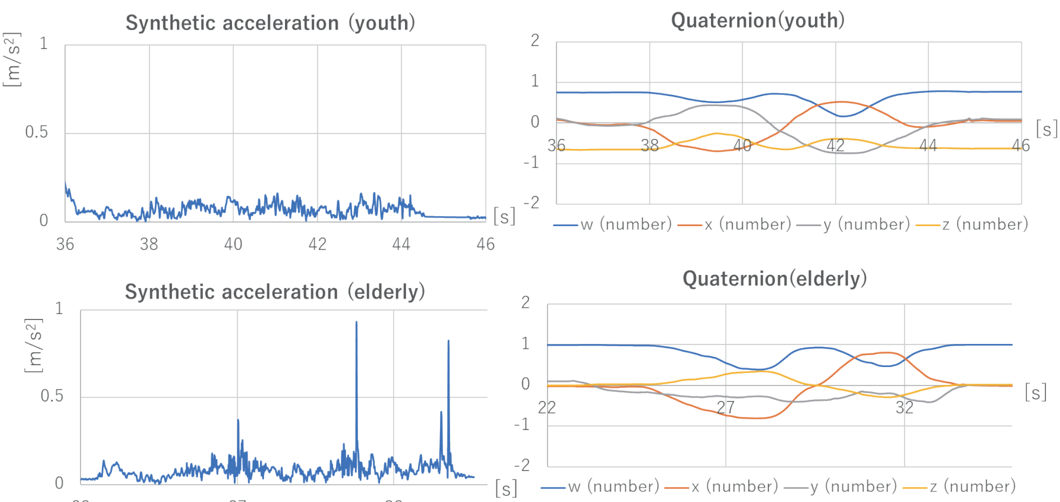

Fig. 10. (Color online) Comparison of waveforms in Exercise F.

Figure 11 shows a histogram and boxplots comparing the composite acceleration averages in the time domain of the measurements of the five exercises performed by elderly people and the corresponding measurements for the young people. A (blue) represents elderly people and B (red) represents young people. First, for Exercise B, the *P*-value is less than 0.001 and, as can be seen in the two figures, the acceleration of the young person is significantly larger than that of the elderly person. For Exercise C, the *P*-value less is than 0.001, and the overall difference in the acceleration for the young person is significantly greater than that for the elderly person, as can be seen in the two figures. For Exercise D, the *P*-value is less than 0.001, and the acceleration of

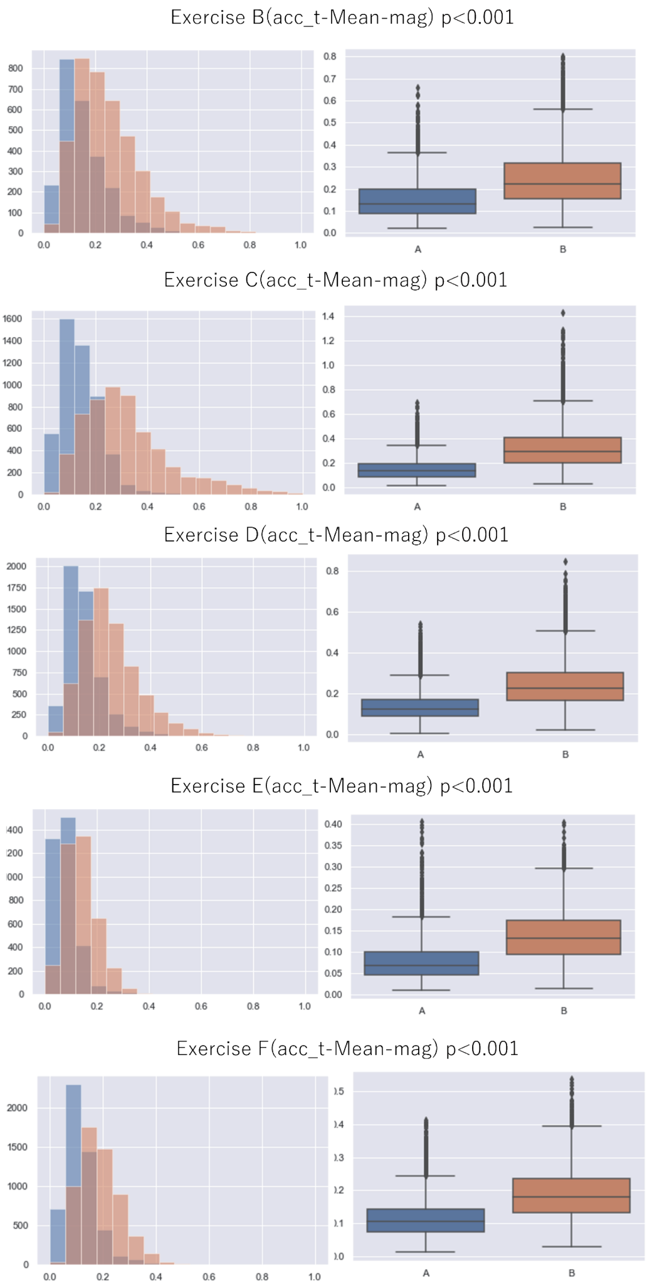

Fig. 11. (Color online) Comparison of the composite acceleration mean (acc_t-Mean-mag) in the time domain for the data of young and elderly people.

the young person is significantly larger than that of the elderly person. For Exercise E, the P-value is less than 0.001 and, similarly to Exercises B to D, the overall difference in acceleration for the young person is significantly larger. Finally, Exercise F has a P-value of less than 0.001, and the acceleration of the young person is also significantly greater than that of the elderly person.

Therefore, the composite acceleration averages in the time domain were confirmed to be effective in determining whether the exercises were performed by young or elderly people.

4.3 Performance evaluation

The performance of the proposed system was evaluated by leave-one-person-out cross-validation using the nine machine learning algorithms described in Sect. 3. Figure 12 shows a bar graph of the F values calculated when all machine learning algorithms were run on the sensor data of the 21 young people. The highest recognition accuracy was achieved using LightGBM, with an F value of 90.0%. In contrast, the lowest recognition accuracy was achieved using NB, with an F value of 52.4%. Figure 13 shows a bar graph of the F values calculated from runs using sensor data from the 14 elderly persons. The highest recognition accuracy was achieved using LightGBM, with an F value of 86.6%. In contrast, the lowest recognition accuracy was achieved using NB, with an F value of 45.2%.

The reason why LightGBM was the most accurate may be that this machine learning algorithm is a combination of the DT algorithm and gradient boosting. Therefore, the proposed method confirms the effectiveness of LightGBM as a machine learning algorithm. Figures 14 and 15 show the confusion matrices resulting from the evaluation using LightGBM, which was the most accurate of the machine learning algorithms, for the data for young and elderly people, respectively.

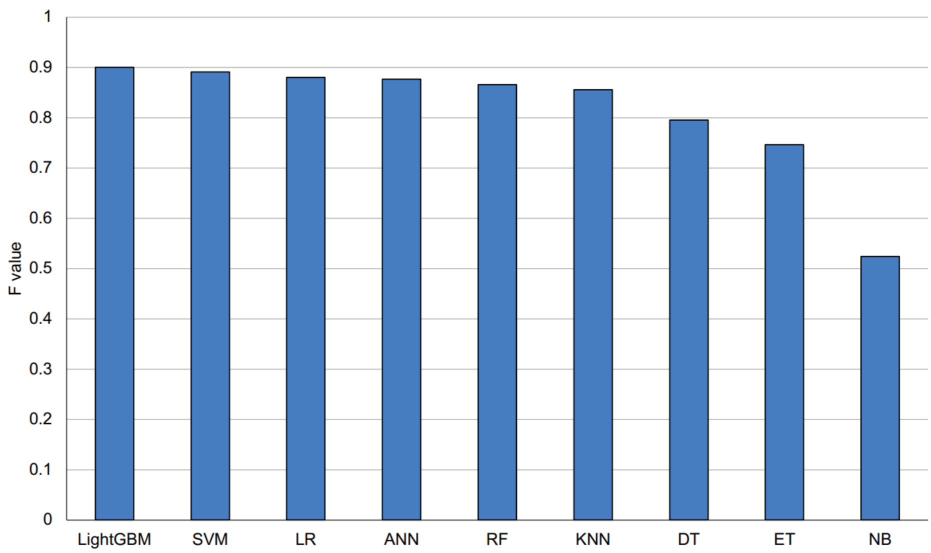

Fig. 12. (Color online) F value results for each machine learning algorithm when using data for young people.

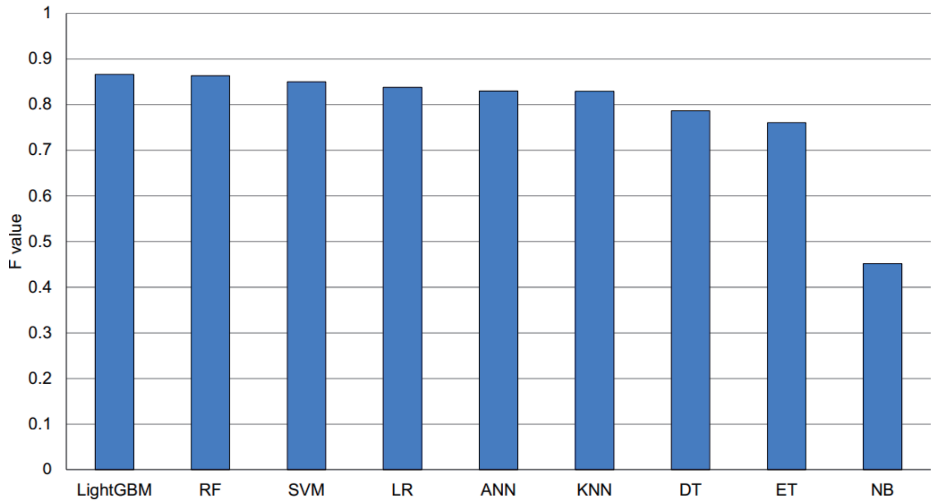

Fig. 13. (Color online) F value results for each machine learning algorithm when using data for elderly people.

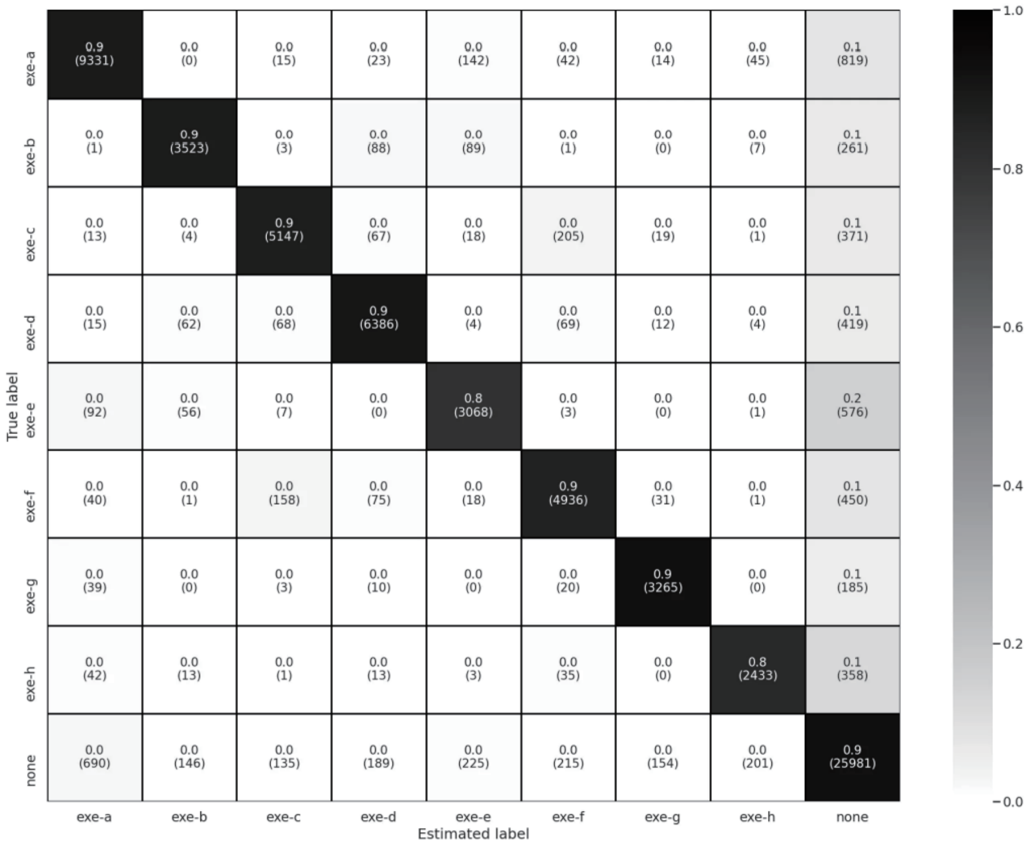

Fig. 14. Performance evaluation of using LightGBM from data for young people.

As can be seen in Fig. 14, for the young people, the overall accuracy of the data is highest when using LightGBM. The accuracy of Exercises A to E was about 86%, which is lower than that of the other exercises. The results were slightly lower than those of a previous study.

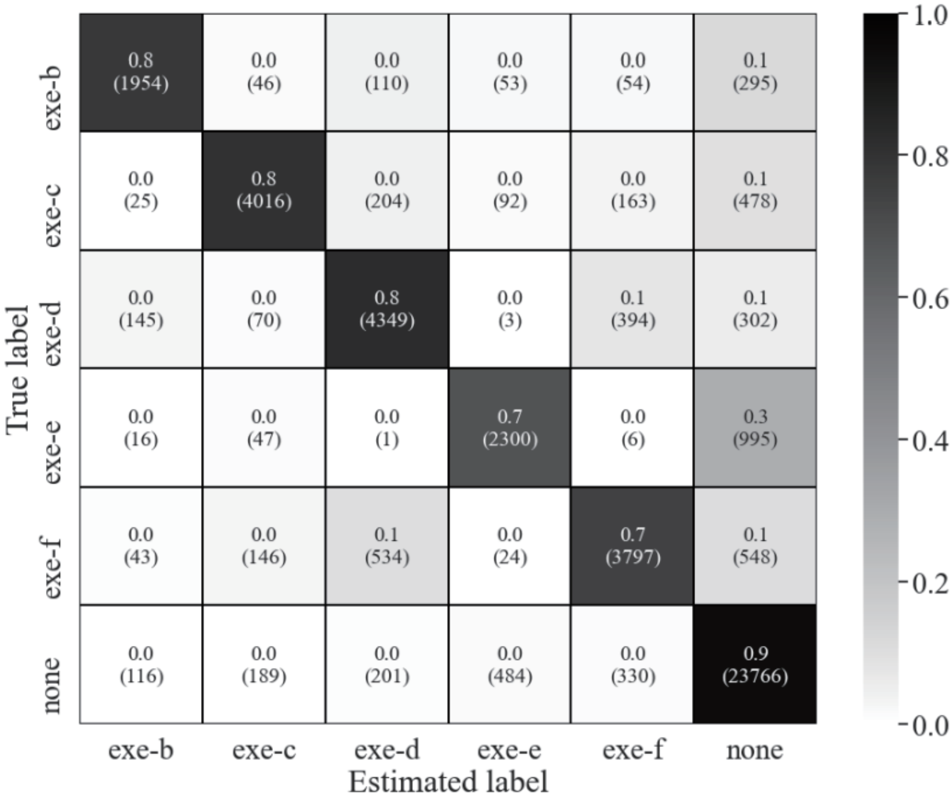

Fig. 15. Performance evaluation of using LightGBM from data for elderly people.

As can be seen in Fig. 15, the results for the elderly people using LightGBM are slightly less accurate than those for the young people: Exercises B to D achieved about 80% accuracy and Exercises E and F achieved about 70% accuracy.

In conclusion, the types of short stick exercises performed by both young and elderly people were recognized with high accuracy using the data. However, some of the exercise events were not correctly identified. This may be due to the fact that many subjects performed the exercises, which created individual differences in movements during exercises. In the future, we would like to improve the proposed method to recognize movements during exercises more accurately.

5. Conclusions

In this paper, we proposed an IMU-based short stick exercise tracking method that can automatically record the type of exercise and the number performed by doing exercises using a short stick equipped with an IMU sensor. The proposed method extracts time-domain and frequency-domain features from the linear acceleration and quaternion time-series data obtained from the IMU and classifies the type of exercise using an inference model based on machine learning algorithms. In our experiment, we evaluated the performance of the proposed method using sensor data that were collected from 21 young people (in their 20s) and 14 elderly people (79–95 years old) for eight basic types of exercise (five types for elderly people). As a result, we confirmed that when LightGBM was used as the learning algorithm in the leave-one-person-out scenario, it achieved high accuracy with *F* values of 90.0 and 86.6% for recognizing the type of exercise for young and elderly people, respectively. The results indicate that our proposed method works well in a variety of short stick exercises for young and elderly people. In the future, we intend to integrate this method into a smartphone application to implement a system that allows users to easily record short stick exercises at home. We also plan to increase the number of types of exercises covered by the proposed method and to study feedback methods to support correct exercising.

Acknowledgments

This research was supported by JST PRESTO (JP-MJPR21P7) and a Grant-in-Aid for Scientific Research (B) (No. 20H04177).

References

1 K. Yokoi, K. Yoshimasu, S. Takemura, J. Fukumoto, S. Kurasawa, and K Miyashita: Disability Rehabil. **37** (2015) 1268. https://doi.org/10.3109/09638288.2014.961660
2 C. Shen, B.-J. Ho, and M. Srivastava: IEEE Trans. Mobile Computing **17** (2017) 1609. https://doi.org/10.1109/TMC.2017.2775641
3 M. Takata, M. Fujimoto, K. Yasumoto, Y. Nakamura, and Y. Arakawa: Proc. 2018 ACM Int. Joint Conf. and 2018 Int. Symp. Pervasive and Ubiquitous Computing and Wearable Computers (2018) 1404–1408. https://doi.org/10.1145/3267305.3267504
4 C. Dobre, L. Bajenaru, I. A. Marinescu, and M. Tomescu: 2019 22nd Int. Conf. Control Systems and Computer Science (CSCS) (IEEE, 2019) 636–642. https://doi.org/10.1109/CSCS.2019.00115
5 A. A. R. Richard, M. F. Sadman, U. H. Mim, I. Rahman, and M. S. R. Zishan: 2019 Int. Conf. Robotics, Electrical and Signal Processing Techniques (ICREST) (IEEE, 2019) 677–681. https://doi.org/10.1109/ICREST.2019.8644452
6 I. Susnea, L. Dumitriu, M. Talmaciu, E. Pecheanu, and D. Munteanu: Sensors **19** (2019) 2264. https://doi.org/10.3390/s19102264
7 R.-A. Voicu, C. Dobre, L. Bajenaru, and R.-I. Ciobanu: Sensors **19** (2019) 458. https://doi.org/10.3390/s19030458
8 O. C. Kurban and T. Yıldırım: IEEE Sens. J. **19** (2019) 7543. https://doi.org/10.1109/JSEN.2019.2915524
9 L. T. Vidal, H. Zhu, and A. Riego-Delgado: Proc. 2020 CHI Conf. Human Factors in Computing Systems (2020) 1–14. https://doi.org/10.1145/3313831.3376268
10 Y. Torigoe, Y. Nakamura, M. Fujimoto, Y. Arakawa, and K. Yasumoto: Sens. Mater. **32** (2020) 651. https://doi.org/10.18494/SAM.2020.2615
11 P. Blank, J. Hoßbach, D. Schuldhaus, and B. M Eskofier: Proc. 2015 ACM Int. Symp. Wearable Computers (2015) 93–100. https://doi.org/10.1145/2802083.2802087
12 U. Jensen, M. Schmidt, M. Hennig, F. A Dassler, T. Jaitner, and B. M. Eskofier: Sports Eng. **18** (2015) 123. https://doi.org/10.1007/s12283-015-0171-9
13 M. Sundholm, J. Cheng, B. Zhou, A. Sethi, and P. Lukowicz: Proc. 2014 ACM Int. Joint Conf. Pervasive and Ubiquitous Computing (2014) 373–382. https://doi.org/10.1145/2632048.2636088
14 S.-P. Lai, C.-A. Hsieh, Y.-H. Lin, T. Harutaipree, S.-C. Lin, Y.-H. Peng, L.-P. Cheng, and M. Y. Chen: 22nd Int. Conf. Human-Computer Interaction with Mobile Devices and Services (2020) 1–8. https://doi.org/10.1145/3379503.3403529
15 Y. Nakamura, Y. Matsuda, Y. Arakawa, and K. Yasumoto: Sensors **19** (2019) 4600. https://doi.org/10.3390/s19204600

About the Authors

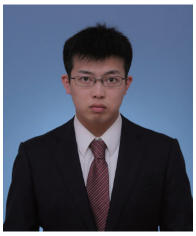

Kazuki Oi received his Bachelor's degree from the National Institute of Technology, Kagawa College, Japan, in 2020 and his master's degree from Nara Institute of Science and Technology, Japan, in 2022. His research interests include information technology and telecommunications engineering. (kazuki.oi@ubi-lab.com)

Yugo Nakamura received his B.E. degree from the Advanced Course of Production System Engineering, National Institute of Technology, Hakodate College, Japan, in 2015 and his M.E. and Ph.D. degrees from the Graduate School of Information Science, Nara Institute of Science and Technology, Japan, in 2017 and 2020, respectively. His current research interests include IoT and ubiquitous computing. He is a member of IEEE, ACM, IPSJ, and IEICE. (y-nakamura@ait.kyushu-u.ac.jp)

Yuki Matsuda received his B.E. degree from the Advanced Course of Mechanical and Electronic System Engineering, National Institute of Technology, Akashi College, Japan, in 2015 and his M.E. and Ph.D. degrees from the Graduate School of Information Science, Nara Institute of Science and Technology, Japan, in 2016 and 2019, respectively. He is currently an assistant professor at the Graduate School of Science and Technology, Nara Institute of Science and Technology. His current research interests include urban sensing, IoT, ubiquitous computing, and affective computing. He is a member of IEEE, IEICE, and IPSJ. (yukimat@is.naist.jp)

Manato Fujimoto received his B.E., M.E., and Ph.D. degrees from Kansai University, Osaka, Japan, in 2009, 2011, and 2015, respectively. From April 2015 to September 2021, he was an assistant professor at the Graduate School of Science and Technology, Nara Institute of Science and Technology. From October 2021 to March 2022, he was an associate professor at the Graduate School of Engineering, Osaka City University. He is currently an associate professor at the Graduate School of Informatics, Osaka Metropolitan University. His research interests include ubiquitous computing, wireless networks, sensing, and monitoring elderly people. He is a member of IEEE, IEICE, and IPSJ. (manato@omu.ac.jp)

Keiichi Yasumoto received his B.E., M.E., and Ph.D. degrees in information and computer sciences from Osaka University, Osaka, Japan, in 1991, 1993, and 1996, respectively. He is currently a professor at the Graduate School of Science and Technology, Nara Institute of Science and Technology, Japan. His research interests include distributed systems, mobile computing, and ubiquitous computing. He is a member of ACM, IPSJ, SICE, and IEICE. (yasumoto@is.naist.jp)